Journal of Electron Spectroscopy and Related Phenomena 184 (2011) 129–133

Contents lists available at ScienceDirect

Journal of Electron Spectroscopy and Related Phenomena

journal homepage: www.elsevier.com/locate/elspec

A VUV photoionization organic aerosol mass spectrometric study with synchrotron radiation

Wenzheng Fang[a], Gong Lei[a], Xiaobin Shan[a], Fuyi Liu[a], Zhenya Wang[b], Liusi Sheng[a,*]

[a] School of Nuclear Science and Technology, National Synchrotron Radiation Laboratory, University of Science and Technology of China, Anhui, Hefei 230029, China
[b] Laboratory of Environmental Spectroscopy, Anhui Institute of Optics and Fine Mechanics, Chinese Academy of Sciences, Hefei 230031, China

ARTICLE INFO

Article history:
Received 17 June 2010
Received in revised form
12 December 2010
Accepted 12 December 2010
Available online 21 December 2010

Keywords:
VUV photoionization
Synchrotron radiation
Organic aerosol
Ionization energy
Ab initio calculations

ABSTRACT

A photoionization aerosol time-of-flight mass spectrometer (ATOFMS) has been developed for on-line analysis of organic compounds in aerosol particles using tunable vacuum ultraviolet (VUV) synchrotron radiation. Aerosol particles can be sampled directly from atmospheric pressure and are focused through an aerodynamic lens assembly into the mass spectrometer. The particles are vaporized when they impact on a heater, and then the nascent vapor is softly photoionized by synchrotron radiation. The degree of fragmentation of molecule can be controlled either by the heater temperature or by the photon energy. Thus, fragment-free tunable VUV mass spectra are obtained by tuning the photon energy close to the ionization energies (IEs) of the sample molecules. The direct determination of the IEs of benzophenone (9.07 eV), salicylic acid (8.72 eV), and urea (9.85 eV) are measured from the photoionization efficiency spectra with uncertainties of ±50 meV. Ab initio calculations have been employed to predict the theoretical ionization energy.

1. Introduction

Primary and secondary organic aerosols (POA and SOA) are ubiquitous throughout the atmosphere environment; both of them have varied chemical compositions as well as diverse physical characteristics that affect the atmospheric chemistry, the earth's climate, visibility, and human health [1–5]. Organic aerosols (OA) make a significant contribution to the total mass of fine aerosols (i.e., PM2.5), contributing ~20 to 50% at continental midlatitudes and up to 90% in tropical forested areas [5]. Although aerosol particles range in diameter from approximately 2 nm to100 μm, the more important particles are ultrafine particles of diameters less than 300 nm since most organic matter exists in much smaller particles [5–7]. In order to understand the formation and reaction mechanism of organic aerosols well, a number of methods are used for on-line and off-line analysis of organic aerosols. Even though real-time analysis of complex organic aerosols is quite difficult and challenging, aerosol mass spectrometry has become a useful analysis tool in testing aerosols in laboratory-based studies, and always combined with varies GC/MS, LC/MS, and FTIR. Comprehensive descriptions of AMS methods and their application to atmospheric science have been given in several reviews [8–12].

Aerosol mass spectrometry (AMS) has been powerfully developed and become an increasingly important analysis tool for its high sensitivity and rapid analysis. However, they still have some limitation in characterizing organic aerosols. One of the main factors in the mass spectrometry of organic aerosols is the method of ionization. Generally, particles enter the mass spectrometers through an aerodynamic lens assembly that effectively transmits particles and focus them into a well-directed tight beam followed by vaporization and ionization of constituents. Inorganic aerosols like salts, nitrate and sulfate can be well analyzed because the most of them are easily vaporized and ionized by ablation with a single UV laser pulse [13,14]. However, the shortcomings of extensive fragmentation of molecules, which come from the multiphoton process by using the high laser power, make distinguishing organic constituents of organic aerosols difficult. In addition, the traditional electron-impact ionization method is also one of the main ionization methods used in the AMS [9–14]. It is usually coupled with a gas or liquid chromatograph. But the electron impact ionization process is often too harsh to preserve molecular structure from organic aerosols. Extensive molecular fragmentation induced by electron impact ionization inevitably

* Corresponding author. Tel.: +86 0551 3602021; fax: +86 0551 5141078.
E-mail address: lssheng@ustc.edu.cn (L. Sheng).

0368-2048/$ – see front matter © 2010 Elsevier B.V. All rights reserved.
doi:10.1016/j.elspec.2010.12.004

results in complicated mass spectra. Even the parent ion peaks of some organic contents do not appear in the mass spectra sometimes. The complicated mass spectra make it extremely difficult to identify the species of complex organic aerosols [15,16]. Single laser desorption/ionization also induces extensive fragmentation of aerosols. Another two-step laser desorption/ionization has been shown to have an advantage in analyzing organic aerosols [11,17]. Using IR laser to vaporize the particles and a UV laser to ionize the nascent vapor subsequently, the AMS offers less fragmentation spectra. Mysak and coworkers coupled synchrotron VUV light with mass spectrometry of aerosols in 2005 [6]. Canagaratna and coworkers reported the results obtained with an aerosol time-of-flight mass spectrometer utilizing two switchable ionization sources, electron impact and VUV radiation generated with a VUV lamp [12].

In this paper, we report a vacuum ultraviolet (VUV) photoionization organic aerosol mass spectrometric study with synchrotron radiation, which are initial results measured with our new home-made VUV photoionization aerosol time-of-flight mass spectrometer (VUV-ATOFMS). The instrument is similar with that Mysak and others reported [6,18,19], and a detailed description of the instrument is discussed below. Here we use the method to introduce solid organic samples into the gas phase via formation of aerosol nanoparticles, followed by thermal vaporization and detection by tunable VUV photoionization mass spectrometry. Benzophenone, salicylic acid are selected because they are the potential products of SOA from the photooxidation of aromatic hydrocarbons. Urea is selected for it can be directly emitted to the atmosphere from anthropogenic and biogenic sources. To our knowledge, even the IE of salicylic acid is unknown. The earlier reported ionization energy (IE) and fragmentation information of benzophenone and urea are too old and need to be updated. Mysak and coworkers have measured the ionization energy of oleic acid using similar method [6]. The fragment-free mass spectra of benzophenone, salicylic acid, urea and oleic acid particles can be obtained by tuning the photon energy to achieve near threshold ionization. The measured ionization energies are compared to ab initio calculations performed by us. The species can be identified by their molecular and fragment ions weights as well as by the comparisons between their theoretical and experimental ionization energies.

2. Experimental

The organic aerosols are generated by the spray method utilizing a dilute solution of the organic molecules with various solvents. The created dry particles using a Constant Output Atomizer (TSI, Inc., model 3076) and Diffusion Dryer (TSI, Inc., model 3062) are directed either into the experimental chamber for mass spectral analysis or into a Scanning Mobility Particle Sizer (SMPS) Spectrometer (TSI, Inc., model 3936) for particle size distribution and number concentration characterization. The SMPS system consists of an electrostatic classifier (TSI, Inc., model 3080) and an ultrafine condensation particle counter (UCPC) (TSI, Inc., model 3776). As the aerosol entered the electrostatic classifier, it is directed into a Kr-85 neutralizer for charge equilibration and then into a long differential mobility analyzer (DMA). Particles are sampled into the mass spectrometer through a 130 μm diameter flow-limiting orifice combined with an aerodynamic lens assembly and a three stage differential pumping system is used to sample them at atmospheric pressure. The aerodynamic lens consists of five apertures that focus particles into a narrow beam. The lens system used here is similar to the one described by Zhang et al. [20]. Fig. 1 shows the schematic diagram of the VUV-ATOFMS instrument constructed at the Atomic and Molecular

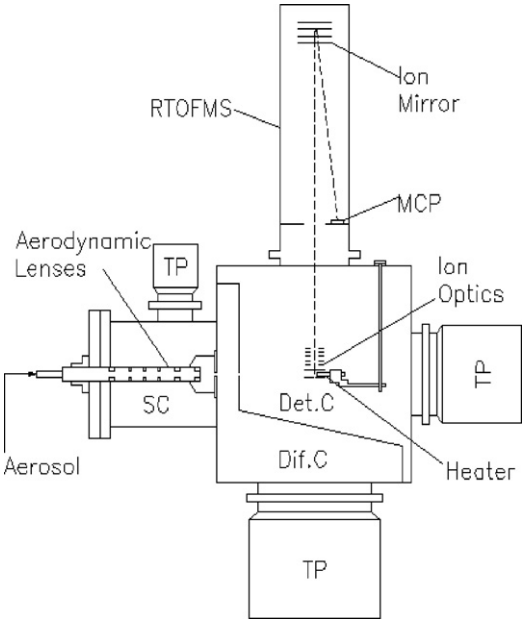

Fig. 1. Vacuum-ultraviolet aerosol time-of-flight mass spectrometer (VUV-ATOFMS). SC, Dif. C, and Det. C stand for the source chamber, the differential chamber, and the detection chamber. TP represents the turbo pump.

Physics Beamline (U14-A) at the National Synchrotron Radiation Laboratory (NSRL) in Hefei, China. The machine is similar with the one constructed at the Chemical Dynamics Beamline at the Advanced Light Source. The source chamber, differential chamber, and detection chamber are collimated to each other. An aperture with a diameter of 3 mm is used to connect the source chamber and the differential chamber, while a 4 mm diameter aperture is used to connect the differential chamber and the detection chamber.

Once transported into the detection chamber, the aerosols are thermally vaporized (up to 873 K) on an 8 mm diameter copper tip inserted between the TOF optics. The nascent vapor expanded back into the source region is photoionized by the tunable vacuum ultraviolet (VUV) synchrotron radiation. SR from an undulator-based U14-A beamline of 800 MeV electron storage ring at the NSRL, is dispersed with a 6 m length monochromator, which is equipped with three gratings (370, 740, and 1250 grooves mm^{-1}, Horiba Jobin Yvon). Three gratings cover the photon energy from 7.5 to 22.5 eV for 370 grooves mm^{-1}, 15 to 45 eV for 740 grooves mm^{-1}, and 36 to 124 eV for 1250 grooves mm^{-1}, respectively. In these experiments, only 370 grooves mm^{-1} grating is used and its energy resolving power ($E/\Delta E$) is above 2000 when the widths of the entrance and exit slits are adjusted to 80 (m. For instance, the energy resolution of photons at 15.9 eV is measured to be 6 meV [full width at half maximum (FWHM)] [21–23], and the newly measured energy resolution is 9 meV from our TPEPICO setup. [24] The average photon flux is about 10^{12} photons s^{-1} and the photon beam spot size is ~500 μm in the region where the photon and particle beam intersect. The absolute wavelength of monochromator is precisely calibrated with the known IEs of inert gases. The synchrotron light is passed through a rare-gas filter to remove high-energy harmonics produced by the undulator. We test the filter factor for high harmonic radiation at photon energy of 12 eV, N_2 (IE = 15.581 eV) is selected as the sample, the suppression efficiency of the rare-gas (Ar) harmonic filter is above 99.9% when the pressure of Ar in the filter is about 5 T (Fig. 2). The ions are detected with a reflectron TOF mass spectrometer. The undulator is contin-

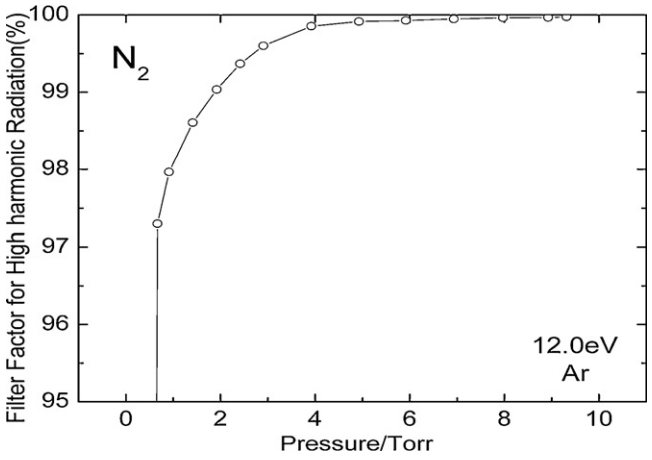

Fig. 2. Filter factor for high harmonic radiation as a function of the pressure of Ar gas harmonic filter at a photon energy 12 eV, N_2 (IE = 15.581 eV) is selected as the sample.

uously scanned and TOF mass spectra are collected in 0.05 eV steps. To normalize the ion signals, the photon intensity is monitored simultaneously with a silicon photodiode (SXUV-100, International Radiation Detectors, Inc.). Photoionization efficiency (PIE) curves can be extracted for each mass after correction for photon flux.

2.1. Quantum chemistry calculations

The geometries of a number of predicted conformers have been fully optimized at the B3LYP/6-311++G theoretical level followed by vibrational analysis [25]. The local adiabatic ionization energy (IEa) of the conformers is calculated according to the following equation: $IEa = E(GS) + ZPE(GS) - E^+(CGS) - ZPE^+(CGS)$, where $E^+(CGS)$ is the total electronic energy of a fully optimized cationic ground state conformer, and $ZPE(GS)$ and $ZPE^+(CGS)$ correspond to the correction values for ground state of the neutral and ionized molecule, respectively. The energies and geometry optimization of ionized conformers (open shell configurations) have been calculated at the same theoretical level utilizing the unrestricted B3LYP/6-311++G (UB3LYP/6-311++G) method.

3. Results and discussion

3.1. Time-of-flight mass spectra

Fig. 3 shows the photoionization mass spectra of benzophenone particles, salicylic acid particles, urea particles, and oleic acid particles. All of them are obtained by varying the ionization energy at the applicable vaporization temperature. The particles are produced by atomizing the solution of 0.3 g benzophenone in 300 ml ethanol, 0.3 g salicylic in 300 ml ethanol, 0.3 g urea in 300 ml ethanol and 0.1% (V/V) oleic acid in isopropyl alcohol. The average diameter of particles is tested to be about 50–120 nm by SMPS. The photoionization mass spectra are remarkably clean at each near threshold energy, showing only minimal fragmentation. By comparison, the standard electron impact mass spectra of all species in this study have much fragment ions peak (see NIST [26]). Similarly, the oleic acid parent ion is only 0.01% as strong as the dominant derived from a parent peak which reported by Morris et al. [27]. As the photon energy is increased, fragmentation of the molecules increases in most cases (Fig. 3). We also find that rais-

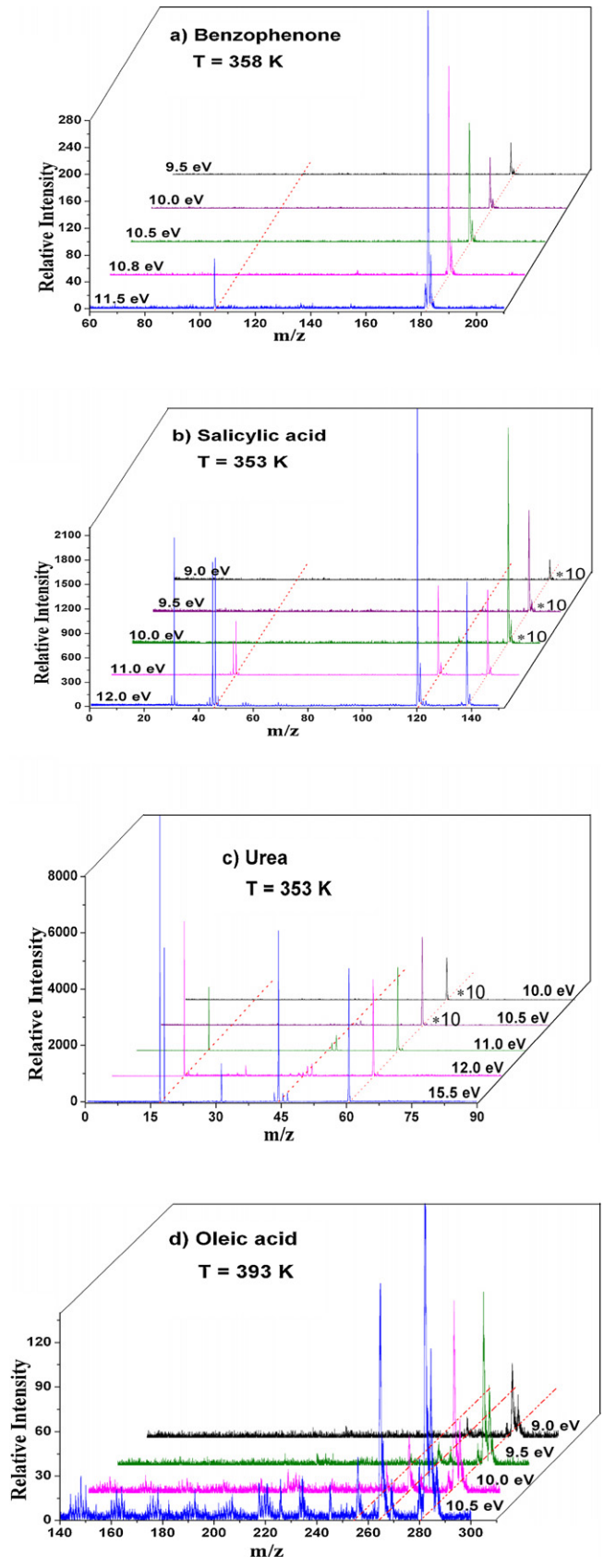

Fig. 3. Mass spectra of benzophenone, salicylic acid, urea, and oleic acid at different VUV photon energies labeled on the figure. The signals of mass spectra are amplified with a factor of 10 at the photon energies of 10.0, 9.5, and 9.0 eV for salicylic acid (b), and are also amplified with a factor of 10 at the 10.5 and 10.0 eV for urea (c), as labeled in their figures.

Table 1
Experimental, theoretical and literature results of ionization energy (IE), appearance energy (AE) in this study.

	IE(exp) (eV)	IE or AE (theo) (B3LYP/6-311++G) (eV)		Ref. (eV)
Benzophenone	9.07	8.52	9.14 (PI)	Iskakov and Potapov (1971) [26]
			9.05 (PE)	McAlduff and Bunbury (1979) [26]
			9.28 (EI)	Elder et al. (1974) [26]
$C_6H_5CO^+$		10.62	12.0 (EI)	Grutzmacher and Schubert (1979) [26]
			11.4 (EI)	Heller, Varmuza (1974) [26]
Urea	9.85	9.55	9.7 (PE)	Debies and Rabalais (1974) [26]
			10.27(EI)	Baldwin et al. (1966) [26]
NH_3		9.98	10.02 (PI)	Qi et al. (1995) [30]
CH_2NO^+		12.62	12.90 (EI)	Loudon and Webb (1977) [31]
Salicylic acid	8.72	8.60		

ing the heater temperature much higher increases the amount of fragmentation in our experiments as shown by Sykes et al. [28] and Nash et al. [29]. Both the lower heater temperature and the lower photon energy can minimize the fragmentation of the parent molecule.

The signals at mass greater than that of parent molecules are not detected in the experiments reported here. We also try to conduct the photoionization measurements with varied pressures of carrier gas, no signals at mass of dimmers or complexes can be found. The nanoparticle source described here has a number of advantages over conventional thermal and laser desorption methods for obtaining fragment-free photoionization mass spectra. Wilson et al. [18] postulated that there are at least three main reasons for this. That is, first, the nanoparticle beam is substrate-free, removing the need to supply additional thermal energy to break intermolecular molecule–substrate bonds. Second, nanoparticles undergo very rapid heating during the short residence times on the heated tip. Last, the nanoparticle morphology (e.g. intermolecular bonding) may play a role in the thermal release of intact molecules into the gas phase. The more polar solvents, like water, increase the amount of intra- and intermolecular hydrogen bonding in the nanoparticle and consequently increase the thermal energy needed to liberate the intact molecule. The larger that the binding energy of the dimer or complex (with solvent) is, the higher temperature it needs to liberate the intact molecule.

The TOF mass spectra of benzophenone (Fig. 3(a)) are obtained by vaporizing its particles at 358 K and photoionizing it at different energies. These spectra are remarkably clean; most of them are dominated by a single peak at 182m/z – corresponding to the benzophenone molecular ion. At 11.5 eV photon energy a second peak appears at 105m/z corresponding to the $C_6H_5CO^+$ produced by the scission of the C–C single bond and elimination phenyl radical. The appearance energy (AE) of $C_6H_5CO^+$ is likely to be around 11.4 eV (Table 1) [26], which may explain that a peak at 105m/z appears at 11.5 eV and vanishes at the lower energies in Fig. 3(a).

Fig. 3(b) shows mass spectra of salicylic acid obtained by vaporizing its particles at 353 K and photoionizing it at 12.0–9.0 eV. The mass spectra contain a water loss peak at 120m/z both at 11.0 and 12.0 eV. Only one peak corresponding to the molecular ion appears at 9.0, 9.5, 10.0 eV.

As shown in Fig. 3(c), the major peak is a fragment ion at m/z 17 at the higher energy of 15.5 eV, followed by the other fragment ion at m/z 44 and parent at m/z 60. The mass peak at mass 17, 44 are assigned to ammonia ion (NH_3^+) and CH_2NO^+. The ionization energy (IE) of NH_3 is about 10.02 eV (Table 1) [26,30]. Whereas, mass peak at mass 17 appears at $\geq$11.0 eV and disappears at $\leq$10.5 eV, this behavior indicates that the AE of NH_3^+ is between 10.5 and 11.0 eV in this study. So the AE of NH_3^+ disagrees with the IE of NH_3. That means the observed fragment m/z 17 probably comes from the dissociation of urea molecular ion, not from the thermal dissociation at the heater followed by photoionization. Fragment m/z 44 appears at 15.5 eV and disappears below 12.0 eV. Previous work shows that the AE of CH_2NO^+ is about 12.9 eV [26,31]. We tentatively assign m/z 44 as CH_2NO^+.

The mass spectra of oleic acid at 10.5 eV and 10 eV shown in Fig. 3(d) contain a water loss peak at 264m/z and an acetylene loss peak at 256m/z. The water loss peak is common characteristic of many organic acids [6,32], similarly in the mass spectra of salicylic acid in Fig. 3(b).

3.2. Ionization energy of benzophenone, salicylic acid, and urea

Fig. 4 shows the photoionization efficiency (PIE) curves for (a) benzophenone (m/z 182) at a heater temperature of 358 K, (b) salicylic acid (m/z 138) at a heater temperature of 353 K, and (c) urea (m/z 60) at a heater temperature of 353 K, respectively. Photoionization efficiency (PIE) curves, acquired by scanning the photon energy, are used to measure the ionization energy for our three compounds. The photon energy is scanned between 8.0 and 12.0 eV, and all mass spectra are collected at a scan step of 0.05 eV. The PIE curves are obtained by measuring TOF spectra as a function of photon energy. Each of them is produced by background correction and normalized with respect to the photon flux. Ar is used as gas filter medium for removing higher order harmonics produced by the undulator, and the pressure of the gas filter chamber is ~5 T. Wilson et al. suggested that increasing the heater temperature did not change the shape of the PIE curve and the ionization energy determination is independent of temperature in their cases [18,19]. The PIE curves of the three sample molecules are used to obtain the ionization energies of 9.07 eV (benzophenone), 8.72 eV (salicylic acid), and 9.85 eV (urea). To our knowledge, this is the first reported ionization energy for salicylic acid. The relatively sharp onsets for salicylic acid and urea suggest that our derived energies for them are close to the adiabatic ionization energies obtained from the B3LYP calculated ones (Table 1). To some extent, fragmentation of molecules during photoionization is an inevitable question when ionizing a low-volatility sample that requires heating in order to vaporize. Fragments may come from the result of neutral dissociation prior to ionization, or come from the result of dissociative photoionization of a hot neutral molecule. However, we cannot find that any of the five stable neutral molecules are fragmented by the heater set up to 393 K in this study.

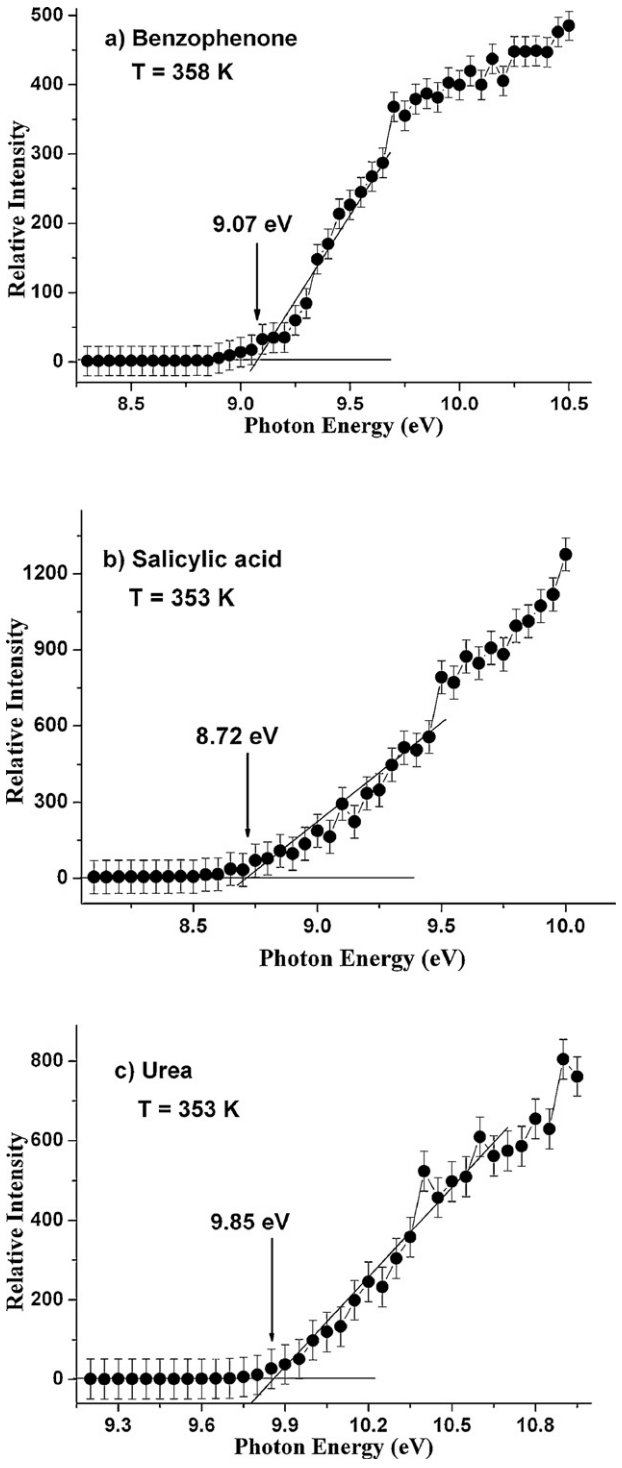

Fig. 4. PIE curves for (a) benzophenone, (b) salicylic acid, and (c) urea.

4. Conclusions

A VUV aerosol mass spectrometric study for several organic particles with tunable synchrotron radiation is presented. The pretty clean mass spectra can obtain by low photon energy photoionization. Moreover, it indicates that the vaporization process with the temperature of a heater up to 393 K does not impart sufficient energy to the molecules to cause much fragmentation. The measured IEs of benzophenone (9.07 eV), salicylic acid (8.72 eV), and urea (9.85 eV) are direct determination from their photoionization efficiency spectra. Ab initio calculation has been employed to predict the theoretical ionization energy and some fragmentation information.

Acknowledgements

This work has been supported by the Knowledge Innovation Foundation of the Chinese Academy of Sciences (KJCX2-YW-N07) and the National Natural Science Foundation of China (No. 10874167).

References

[1] B. Warscheid, T. Hoffmann, Rapid Commun. Mass Spectrum. 15 (2001) 2259.
[2] M.O. Andreae, P. Crutzen, Science 276 (1997) 1052.
[3] C.E. Corrigan, T. Novakov, Atmos. Environ. 33 (1999) 2661.
[4] Y. Rudich, Chem. Rev. 103 (2003) 5097.
[5] H. John, Seinfeld, N. Spyros, Pandis, Atmospheric Chemistry and Physics: From Air Pollution to Climate chAnge, 2nd ed., Wiley, Hoboken, NJ, 2006.
[6] E.R. Mysak, K.R. Wilson, M. Jimenez-Cruz, M. Ahmed, T. Baer, Anal. Chem. 77 (2005) 5953.
[7] B.J. Turpin, P. Saxena, E. Andrews, Atmos. Environ. 34 (2000) 2983–3013.
[8] Scott Geddes, Brian Nichols, Brian Nichols, Stevenson Flemer Jr., Jessica Eisenhauer, James Zahardis, Giuseppe A. Petrucci, Anal. Chem. 82 (2010) 7915.
[9] J.T. Jayne, D.C. Leard, X.F. Zhang, P. Davidovits, K.A. Smith, C.E. Kolb, D.R. Worsnop, Aerosol Sci. Technol. 33 (2000) 49–70.
[10] D.G. Nash, T. Baer, M.V. Johnston, Int. J. Mass Spectrom. 258 (2006) 2–12.
[11] R.C. Sullivan, K.A. Prather, Anal. Chem. 77 (2005) 3861–3886.
[12] M.R. Canagaratna, J.T. Jayne, J.L. Jimenez, J.D. Allan, M.R. Alfarra, Q. Zhang, T.B. Onasch, F. Drewnick, H. Coe, A. Middlebrook, A. Delia, L.R. Williams, A.M. Trimborn, M.J. Northway, P.F. DeCarlo, C.E. Kolb, P. Davidovits, D.R. Worsnop, Mass Spectrom. Rev. 26 (2007) 185–222.
[13] B.A. Mansoori, M.V. Johnston, A.S. Wexler, Anal. Chem. 66 (1994) 3681–3687.
[14] E. Gard, J.E. Mayer, B.D. Morrical, T. Dienes, D.P. Fergenson, K.A. Prather, Anal. Chem. 69 (1997) 4083.
[15] M.R. Canagaratna, J.T. Jayne, D.A. Ghertner, S. Scott, Q. Shi, J.L. Jimenez, P.J. Silva, P. Williams, T. Lanni, F. Drewnik, K.L. Demerjian, C.E. Kolb, D.R. Worsnop, Aerosol Sci. Technol. 38 (2004) 555–573.
[16] J.L. Jimenez, J.T. Jayne, Q. Shi, C.E. Kolb, D.R. Worsnop, I. Yourshaw, J.H. Seinfeld, R.C. Flagan, X. Zhang, K.A. Smith, J.W. Morris, P.J. Davidovits, J. Geophys. Res. 108 (2003), SOS 13/1-SOS 13/13.
[17] A. Zelenyuk, D. Imre, Aerosol Sci. Technol. 39 (2005) 554–568.
[18] K.R. Wilson, M. Jimenez-Cruz, C. Nicolas, L. Belau, S.R. Leone, M. Ahmed, J. Phys. Chem. A 110 (2006) 2106.
[19] R.W. Kevin, Leonid Belau, Christophe Nicolas, Michael Jimenez-Cruz, R.L. Stephen, Ahmed Musahid, Int. J. Mass Spectrom. 249–250 (2006) 155.
[20] X. Zhang, K.A. Smith, D.R. Worsnop, J. Jimenez, J.T. Jayne, C.E. Kolb, Aerosol Sci. Technol. 36 (2002) 617.
[21] S.S. Wang, R.H. Kong, X.B. Shan, Y.W. Zhang, L.S. Sheng, Z.Y. Wang, L.Q. Hao, S.K. Zhou, J. Synchrotron Radiat. 13 (2006) 415.
[22] Yujie Zhao, Yue Sun, Jinda Sun, Wenzheng Fang, Xiaobin Shan, Fuyi Liu, Liusi Sheng, Zhenya Wang, J. Electron Spectrosc. Relat. Phenom. 173 (2009) 24–28.
[23] L. Gong, W.Z. Fang, F.Y. Liu, X.B. Shan, L.S. Sheng, Z.Y. Wang, J. Electron Spectrosc. Relat. Phenom. 182 (2010) 134–140.
[24] Xiaofeng Tang, Xiaoguo Zhou, Mingli Niu, Shilin Liu, Jinda Sun, Xiaobin Shan, Fuyi Liu, Liusi Sheng, Rev. Sci. Instrum. 80 (2009) 113101.
[25] M.J. Frisch, G.W. Trucks, H.B. Schlegel, G.E. Scuseria, M.A. Robb, J.R. Cheeseman, J.A. Montgomery, Jr., T. Vreven, K.N. Kudin, J.C. Burant, J.M. Millam, S.S. Iyengar, J. Tomasi, V. Barone, B. Mennucci, M. Cossi, G. Scalmani, N. Rega, G.A. Petersson, H. Nakatsuji, M. Hada, M. Ehara, K. Toyota, R. Fukuda, J. Hasegawa, M. Ishida, T. Nakajima, Y. Honda, O. Kitao, H. Nakai, M. Klene, X. Li, J.E. Knox, H.P. Hratchian, J.B. Cross, C. Adamo, J. Jaramillo, R. Gomperts, R.E. Stratmann, O. Yazyev, A.J. Austin, R. Cammi, C. Pomelli, J.W. Ochterski, P.Y. Ayala, K. Morokuma, G.A. Voth, P. Salvador, J.J. Dannenberg, V.G. Zakrzewski, S. Dapprich, A.D. Daniels, M.C. Strain, O. Farkas, D.K. Malick, A.D. Rabuck, K. Raghavachari, J.B. Foresman, J.V. Ortiz, Q. Cui, A.G. Baboul, S. Clifford, J. Cioslowski, B.B. Stefanov, G. Liu, A. Liashenko, P. Piskorz, I. Komaromi, R.L. Martin, D.J. Fox, T. Keith, M.A. Al-Laham, C.Y. Peng, A. Nanayakkara, M. Challacombe, P.M.W. Gill, B. Johnson, W. Chen, M.W. Wong, C. Gonzalez, J.A. Pople, Gaussian, Inc., Pittsburgh PA, 2003.
[26] NIST Chemistry Webbook, National Institute of Standards and Technology, Gaithersburg, MD, 2010. http://webbook.nist.gov/chemistry/.
[27] J.W. Morris, P. Davidovits, J.T. Jayne, Q. Shi, C.E. Kolb, D.R. Worsnop, W.S. Barney, J. Jimenez, G.R. Cass, Geophys. Res. Lett. 29 (2002), 71/1–71/4.
[28] C. Sykes, E. Woods III, G.D. Smith, T. Baer, R.E. Miller, Anal. Chem. 73 (2001) 2048–2052.
[29] D.G. Nash, X.F. Liu, E.R. Mysak, T. Baer, Int. J. Mass Spectrom. 241 (2005) 89–97.
[30] F. Qi, L. Sheng, Y. Zhang, S. Yu, W.-K. Li, Chem. Phys. Lett. 234 (1995) 450.
[31] A.G. Loudon, Org. Mass Spectrom. 12 (1977) 283.
[32] F.W. McLafferty, F. Turecek, Interpretation of Mass Spectra, 4 ed., University Science Books, Sausalito, CA, 1993.